ARTICLE NO. 78-1608R

Particulate Release Rates from Shuttle Orbiter Surfaces Due to Meteoroid Impact

J. Barengoltz*
Jet Propulsion Laboratory, California Institute of Technology, Pasadena, Calif.

An estimate of the magnitude of released particles in the vicinity of a Shuttle Orbiter due to meteoroid impact has been completed. A calculation of the number of particles existing as surface contamination and released by such impacts has been performed. In addition, two estimates of the creation of new particles due to meteoroid cratering (backsplash) have been obtained. In each case, the total number of particles per day as a function of size without regard to velocity, as a function of velocity without regard to size, and as a joint distribution in size and velocity has been calculated.

Introduction

IN the 1980's and beyond, the Space Transportation System (STS), or Shuttle, will be employed to launch virtually all U.S. satellites, spacecraft, and scientific payloads into space. An area of intense interest to the payload community is the potential contamination environment of this new system. Since satellites and spacecraft may be launched in the Orbiter bay without aerodynamic shrouds, they may be exposed to the local contamination environment outside the Orbiter during deployment at orbital altitudes. Scientific payloads for which the Orbiter is to be used as a platform will be exposed to this environment during the entire orbital mission phase.

One source of particulate contamination is micrometeoroid impacts on the external surfaces of the Orbiter. This research was motivated by previous work[1] related to Viking, which treated the release of pre-existing particulates from spacecraft surfaces by this effect. It is expected that the Orbiter, a reusable vehicle, will have a relatively dirty exterior surface. In addition, the creation of new particles from the cratering (pitting) of the glassy surfaces of the special thermal insulation of the orbiter was first treated in the study reported here.

Models

Impact

The impact analysis estimates the number of pre-existing contaminant particles that will be removed due to surface accelerations resulting from meteoroid impact. The analysis consists of a meteoroid model, a surface response model, a surface contamination model, and a particle adhesion model. The analysis was conducted in an analogous manner to the previous calculations performed under the postlaunch recontamination studies.

The meteoroid flux model was adapted from the literature[2] as in the previous work.[1] The total surface area of the Orbiter was taken to be 1200 m^2, of which one-half was struck by meteoroids, an anisotropy due to the Earth's shadow. The model is summarized in Table 1.

Presented as Paper 78-1608 at the AIAA/IES/ASTM 10th Space Simulation Conference, Bethesda, Md., Oct. 16-18, 1978; submitted Dec. 7, 1978; revision received April 10, 1979.

Index categories: Meteoroid and Radiation Protection; Spacecraft Simulation.

*Member of Technical Staff, Applied Mechanics Technology.

The meteoroid impact surface response model was also taken without change from the previous work.[1] It was run for each meteoroid mass group on a set of surface physical parameters that simulated the STS Orbiter's reusable thermal insulation. The values used were a density of 144 kg/m^3, thickness of 3.8×10^{-2} m, elastic modulus of 3×10^5 N/m^2, and compressive yield strength of 6×10^8 N/m^2. (The results are not extremely sensitive to these values.)

Finally, the particle adhesion and surface contamination models were adapted from the previous work.[1] As before, only 10-100 μm particles were considered. This range was justified on the expected distribution cutting off at large sizes, due to aerodynamic removal during launch and the negligible removal of very small particles during meteoroid impact. An arbitrary contamination level of 10^6 particles/m^2 of size 5 μm or larger was assumed (ten times higher than the previous work[1]). Note that the results scale linearly in this parameter.

Spall

The spall analysis estimates the number of particles that will be created and ejected during crater formation following meteoroid impact. There are two versions of this analysis, depending on two distinct assumed size or mass distributions for these particles. The meteoroid flux model was unchanged from that described in Table 1. The surface response, particle adhesion, and surface contamination models were not used, as they do not apply.

The crux of the analysis is the formation of ejecta during cratering. A simpler place to start is with the crater itself. A typical assumption for the crater volume V_c is

$$V_c = E_o/S \tag{1}$$

where E_0 is the meteoroid kinetic energy and S is a yield

Table 1 Meteoroid model parameters

Mass, kg	Velocity, m/s	Flux, $m^{-2}s^{-1}$	Number of hits, day^{-1}
.30−13	.16+05	.10−04	.36+03
.10−12	.16+05	.42−05	.14+03
.10−11	.16+05	.59−05	.20+03
.10−10	.16+05	.28−05	.98+02
.10−09	.16+05	.97−06	.34+02
.10−08	.16+05	.24−06	.83+01
.10−07	.16+05	.47−07	.16+01
.10−06	.16+05	.29−08	.10+00
.10−05	.16+05	.18−09	.62−02

strength of the struck material,[3] or, assuming a hemispherical crater of radius R_c,

$$R_c/d_p = \tfrac{1}{2}(\rho_p v_o^2/S)^{1/3} \quad (2)$$

where d_p is the meteoroid diameter, v_0 is the meteoroid velocity, and ρ_p is the meteoroid density.[1,4,5] Ludloff[4] uses the product of the latent heat of fusion and the density of the target for S.

Other authors[6,7] employ Eq. (1) with factors involving the ratio of the meteoroid to target densities (ρ_p/ρ_t) to some power, typically unity or less, and an empirical constant (also bounded by unity). Bjork[8] has reviewed the problems associated with this sort of simple model. However, for $\rho_p < \rho_t$, Eq. (1) certainly represents an upper limit for V_c.

The assumption of a hemispherical crater may also be attacked. Gault found that R_c was about twice the depth of the crater for impacts in crystalline rocks with projectile mass, velocity, and energy in the meteoroid range.[9] For such a spherical segment (crater), given Eq. (2), Eq. (1) would overestimate the crater volume by a factor of 2.5.

Gault's results may apply to the case at hand, because the thin borosilicate layer on the Orbiter thermal insulation is also a brittle material. (The typical target material of the other researchers was ductile, i.e., a metal.) Nearly all of the ejected material will arise from this glassy coating. For meteoroids large enough to penetrate the coating, the spallation will be driven into the underlying low-density glass foam insulation and will not be ejected.

At this point, an upper limit to the ejected mass M_E may be written as the mass of the crater, $\rho_t V_c$, plus the mass of the meteoroid M:

$$M_E \leq M + \rho_t M v_o^2/2S \quad (3)$$

The physical parameters used for the coating are: density ρ_t, 2400 kg/m^3; thickness, 3×10^{-4}m; yield strength S, 6×10^8N/m^2; and a typical grain size of 4 μm. These values limit the nonpenetrating meteoroid masses to the first five mass groups used in impact analysis (see Table 1). For these values and a meteoroid density ρ_p of about 600 kg/m^3 and velocity of 1.6×10^4 m/s, the meteoroid mass M is negligible to the mass of the rest of the ejecta (Eq. 3).

The rest of Eq. (3) may then be written as

$$M_E \leq 4000\, E_o \quad (4a)$$

where M is expressed in picograms and E_o in microjoules. This departure from MKS units is taken to allow a comparison with Gault's result[9] for these density values:

$$M_E = 590\, E_o^{1.333} \quad (4b)$$

Mandeville and Vetter,[10] working with glass targets, but at projectile kinetic energies below 1 μJ, found

$$M_E = 230\, E_o^{1.1} \quad (4c)$$

In order to bound the conservatism of Eq. (4a), consider the ejected mass M_E times the hit rate for meteoroids in each of the first five groups of Table 1. Clearly, the heavier meteoroids contribute the most. Based on the 1×10^{-10} kg meteoroids, which are at the penetration limit and have an energy of 1.3×10^4 μJ, Eq. (4a) predicts 5.2×10^7 pg, about twice the prediction of Eq. (4b) and seven times the prediction of Eq. (4c).

To proceed, it was assumed that one-half of the meteoroid kinetic energy E_o appears as the total kinetic energy of the ejecta.[5] From this assumption, the total momentum of the ejecta P_E may be written:

$$P_E = E_o\sqrt{\rho_t/S} \quad (5)$$

Table 2 Size distribution, all velocities/impact

Size range, μm	Number, day^{-1}
5 – 15	.328 + 03
15 – 25	.288 + 03
25 – 35	.403 + 03
35 – 45	.508 + 03
45 – 55	.591 + 03
55 – 65	.654 + 03
65 – 75	.701 + 03
75 – 85	.733 + 03
85 – 95	.755 + 03
95 – 105	.767 + 03

Table 3 Size distribution, all velocities/spall

Size range, μm	Number, day^{-1}	
	Model M	Model G&H
1 – 2	.208 + 05	0
2 – 4	.377 + 06	.126 + 08
4 – 6	.689 + 05	.870 + 06
6 – 10	.434 + 05	.264 + 06
10 – 20	.139 + 06	.298 + 06
20 – 40	.504 + 05	.309 + 05
40 – 60	.157 + 05	.215 + 04
60 – 100	.704 + 01	.679 + 03
100 – 200	0	.531 + 03

as well as the average velocity $\bar{v}$ of the ejecta

$$\bar{v} = \sqrt{S/\rho_t} = 500 \text{ m/s} \quad (6)$$

Note that $\bar{v}$ is independent of M. Equations (5) and (6) depend on neglecting the meteoroid mass in Eq. (3).

The analysis can proceed no farther without an average mass for the set of ejected particles, $\bar{m}$, a mass or size distribution, and a velocity distribution. A value for $\bar{m}$ is especially critical, since the total number of ejected particles N is given by

$$N = M_E/\bar{m} \quad (7)$$

Choices for $\bar{m}$, or the average size, include the order of magnitude of the grain size (1 μm) and the size where the surface tension of a molten sphere equals the thermal energy (~2 μm) as minima and the spacing between the meteoroid and the crater, d_{max}, given by

$$d_{max} = 2R_c - d_p \quad (8)$$

as the maximum (see Eq. 2). In reality, $\bar{m}$ should lie between these corresponding limits and depend on the meteoroid parameters (M and v_o).

A reasonable continuation is to assume that the ejecta follow a Maxwell distribution in momentum p; that is,

$$\frac{dN}{dp} = \frac{32}{\pi^2 p_o^3} p^2 \exp\left(-\frac{4p^2}{\pi p_o^2}\right) \quad (9)$$

with $p_o = \bar{m}\bar{v}$. Now, if $\bar{m}$ and a distribution in mass are selected, the distribution in velocity may be obtained.

In particular, in the analysis reported here, two distinct mass or size distributions have been considered; the results of both will be presented.

The first mass distribution, noted by (M) in the results for Maxwell, was constructed by adopting the momentum distribution (Eq. 9) at the average velocity $\bar{v}$. Thus,

$$\frac{dN}{dm}(\bar{v}) = \frac{32}{\pi^2 \bar{m}^3} m^2 \exp\left(-\frac{4m^2}{\pi \bar{m}^2}\right) \quad (10)$$

Equation (10) is properly normalized for $0 \leq m < \infty$. However, in this analysis, a pseudo-Maxwell distribution was formed by constraining m to lie between the mass corresponding to 1 μm and the mass corresponding to d_{max} (Eq. 8). The distribution was then renormalized on this interval.

The value for $\bar{m}$ was selected on the basis of an assumed difference between the depth of melting and the depth of the impact crater. From Bjork et al.,[11] this difference is expected to be $0.2\,R_c$, yielding

$$\bar{m} = (\pi/6)\rho_t (0.2R_c)^3 = 2 \times 10^{-3} \rho_t V_c \qquad (11)$$

From the last version of Eq. (11), it follows that the number of released particulates from a given impact (neglecting the meteoroid mass itself) is approximately 500.

The second mass distribution was based on an experimental size distribution for basalt rock due to Gault and Heitowit.[5]

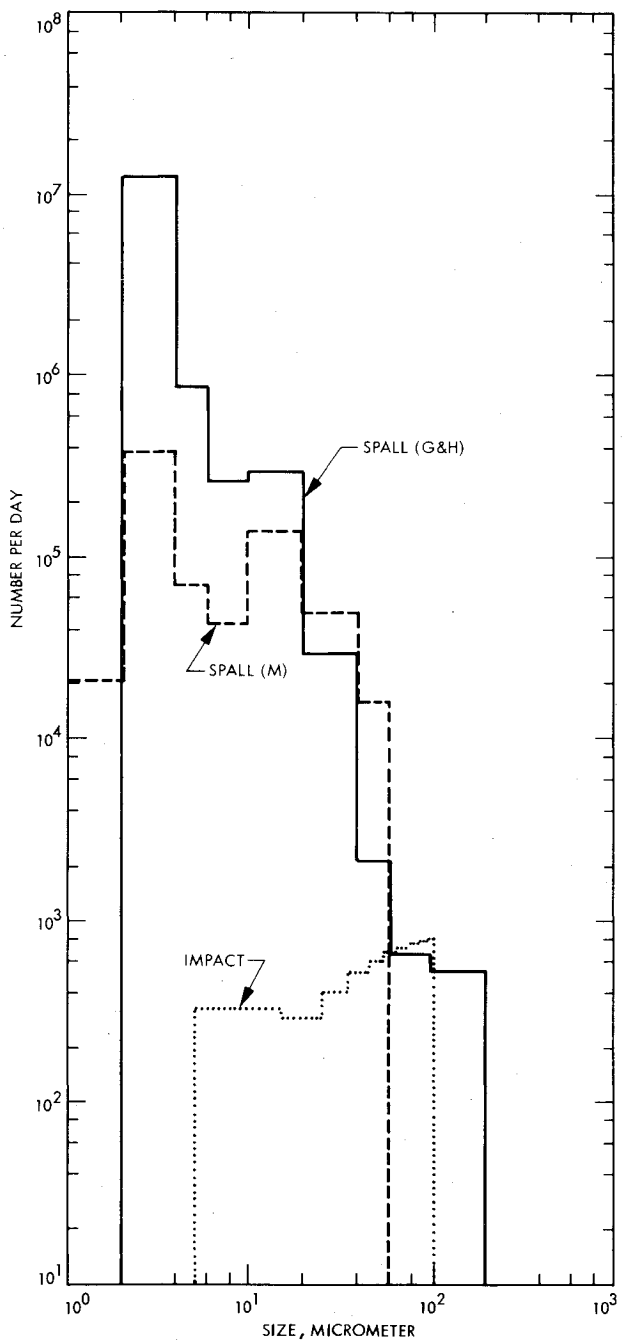

Fig. 1 The distribution of particulates per day caused by meteoroid impact as a function of size irrespective of velocity.

The results from this distribution are denoted by (G&H). In the present adaptation, the sizes (or masses) of ejected particles are bounded to the same interval as in the previous development. In addition to these two parameters, $l_o = 1$ μm and $L = d_{max}$, a third parameter α, determined to be about 0.5 by Gault and Heitowit, was employed. The parameter α is equivalent to a choice of $\bar{m}$, as will be shown.

Table 4 Velocity distribution, all sizes/impact

Velocity range, m/s	Number, day^{-1}
.1 − 04 − .2 − 04	.330-01
.2 − 04 − .4 − 04	.200 + 00
.4 − 04 − .6 − 04	.421 + 00
.6 − 04 − .1 − 03	.793 + 00
.1 − 03 − .2 − 03	.789 + 01
.2 − 03 − .4 − 03	.305 + 02
.4 − 03 − .6 − 03	.529 + 02
.6 − 03 − .1 − 02	.138 + 03
.1 − 02 − .2 − 02	.223 + 03
.2 − 02 − .4 − 02	.418 + 03
.4 − 02 − .6 − 02	.300 + 03
.6 − 02 − .1 − 01	.540 + 03
.1 − 01 − .2 − 01	.740 + 03
.2 − 01 − .4 − 01	.964 + 03
.4 − 01 − .6 − 01	.650 + 03
.6 − 01 − .1 + 00	.372 + 03
.1 + 00 − .2 + 00	.416 + 03
2 + 00 − .4 + 00	.261 + 03
.4 + 00 − .6 + 00	.188 + 03
.6 + 00 − .1 + 01	.707 + 02
.1 + 01 − .2 + 01	.135 + 03
.2 + 01 − .4 + 01	.401 + 02
.4 + 01 − .6 + 01	.785 + 01
.6 + 01 − .1 + 02	.820 + 01
.1 + 02 − .2 + 02	.423 + 01
.2 + 02 − .4 + 02	.461 + 00
.4 + 02 − .6 + 02	.544 + 02
.6 + 02 − .1 + 03	.347 − 01

Table 5 Velocity distribution, all sizes/spall

Velocity range, m/s	Number, day^{-1}	
	Model M	Model G&H
.1 − 01 − .2 − 01	0	.114 + 02
.2 − 01 − .4 − 01	0	.102 + 03
.4 − 01 − .6 − 01	0	.130 + 03
.6 − 01 − .1 + 00	0	.268 + 03
.1 + 00 − .2 + 00	.109 − 03	.119 + 03
.2 + 00 − .4 + 00	.283 − 02	.322 + 03
.4 + 00 − .6 + 00	.142 − 01	.499 + 03
.6 + 00 − .1 + 01	.130 + 00	.172 + 04
.1 + 01 − .2 + 01	.110 + 00	.105 + 04
.2 + 01 − .4 + 01	.286 + 01	.466 + 04
.4 + 01 − .6 + 01	.143 + 02	.916 + 04
.6 + 01 − .1 + 02	.129 + 03	.350 + 05
.1 + 02 − .2 + 02	.107 + 03	.148 + 05
.2 + 02 − .4 + 02	.234 + 04	.628 + 05
.4 + 02 − .6 + 02	.851 + 04	.705 + 05
.6 + 02 − 1 + 03	.399 + 05	.136 + 06
.1 + 03 − .2 + 03	.238 + 05	.558 + 05
.2 + 03 − .4 + 03	.113 + 06	.136 + 06
.4 + 03 − .6 + 03	.142 + 06	.210 + 06
.6 + 03 − .1 + 04	.265 + 06	.701 + 06
.1 + 04 − .2 + 04	.554 + 05	.406 + 06
.2 + 04 − .4 + 04	.369 + 05	.161 + 07
.4 + 04 − .6 + 04	.133 + 05	.252 + 07
.6 + 04 − .1 + 05	.122 + 05	.601 + 07
.1 + 05 − .2 + 05	.147 + 04	.146 + 07
.2 + 05 − .4 + 05	.292 + 03	.645 + 06
.4 + 05 − .6 + 05	.284 + 02	.140 + 05
.6 + 05 − .1 + 06	.129 + 02	.307 + 02
.1 + 06 − .2 + 06	.352 − 01	.208 − 07

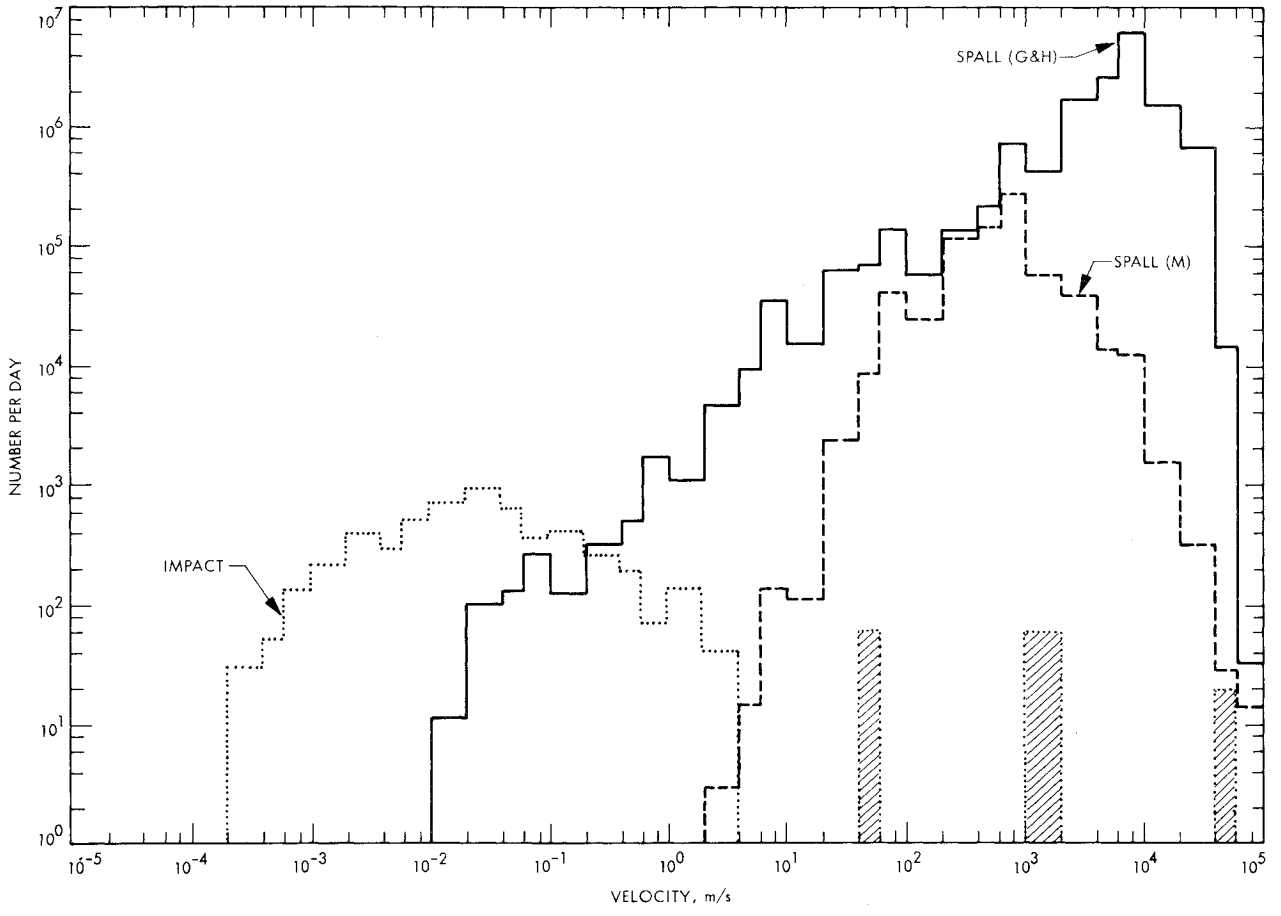

Fig. 2 The distribution of particulates per day caused by meteoroid impact as a function of velocity irrespective of size. (The notation is the same as Fig. 1.)

The distribution in size l may be written

$$\frac{dN}{dl} = \frac{6\alpha M_E}{\pi L^{\alpha}\rho_t l^3}(l-l_o)^{\alpha-1} \tag{12}$$

Since Eq. (12) may be integrated from l_o to L to obtain $N(\leq L)$, the total number of particulates, the average mass $\bar{m}$ may be written

$$\bar{m} = \frac{\pi L^{\alpha}\rho_t}{6\alpha}\left[\int_{l_o}^{L} dl \frac{(l-l_o)^{\alpha-1}}{l^3}\right]^{-1} \tag{13}$$

For the particular parameter values used in this analysis,

$$\bar{m} = (8/9)\rho_t L^{1/2} l_o^{5/2} \tag{14}$$

In this formulation, the average mass $\bar{m}$ depends very weakly on the meteoroid mass M (to the one-sixth power) compared to the previous treatment (proportional to M).

Results and Discussion

The number distributions of particles due to meteoroid impact-induced release and the two cratering analyses are presented as a function of particle size in Tables 2 and 3. These distributions are also shown graphically in Fig. 1.

In the case of meteoroid impact-induced release (labeled "IMPACT" in Fig. 1), the small meteoroids, which are very numerous, remove most of the large particles but few of the small, tightly adhered particles. The larger meteoroids, of which fewer occur, efficiently remove the smaller particles, of which there are many. These competing factors tend to cancel, except that any meteoroid will remove the larger particles. Thus, the results reflect only a gradual increase in the number of particles as a function of increasing size.

Many more particles of any size are produced by the backsplash† mechanism (labeled "SPALL" in Fig. 1), because the crater volume far exceeds the volume of material available in the impact-induced release process. Based on experimental cratering data, backsplash should be heavily biased toward small particles. This effect is reflected in the results.

To a large extent, the number distributions vs particle size are insensitive to the choices of average mass and mass distribution. The principal difference is that the Gault and Heitowit type of size distribution[5] (labeled G&H in Fig. 1) tends to emphasize very large and very small particles compared to the pseudo-Maxwell mass distributions (labeled M). There is a serious spread in the 2-10 μm particle range. However, the average mass parameter itself, as discussed previously, has an overwhelming effect on the total number of particles created by cratering. Thus, these values are very uncertain and must be used with caution.

The number distributions of particles due to meteoroid impact-induced release and the two backsplash analyses are presented as a function of particle velocity in Tables 4 and 5. These distributions are also shown graphically in Fig. 2.

The released particulate distribution is fairly smooth with a peak at about 3 cm/s. This result follows from the extended surface response, which samples the various sizes of released particles with a monotonic smooth velocity profile. The anomalous peaks (crosshatched in Fig. 2) at high velocities are artifactual in the sense that they reflect the graininess of the surface response calculation very close to the crater. However, such particles are real and are small fast particles arising from near the crater. They will, in fact, be spread more evenly over the high-velocity (> 1 m/s) intervals.

The backsplash particle distributions exhibit much higher

†This terminology is apparently due to Eichelberger and Gehring.[12]

velocities than the released particles. This result follows from the considerably higher energy transfer efficiency of the backsplash mechanism, where one-half of the meteoroid kinetic energy appears as ejecta kinetic energy. Although it is possible for some small particles to be ejected at velocities higher than the meteoroid velocity (1.6×10^4 m/s), the distribution drops off above this value, as expected. The distribution resulting from the Gault and Heitowit size model[5] reflects the enhanced numbers of large, low-velocity particles and the greatly enhanced numbers of small, high-velocity particles compared to the pseudo-Maxwell model. The small (≤ 2 μm) particles in the former case make a large contribution at and near the meteoroid velocity. In the latter case, the distribution peaks near 500 m/s as predicted in the Models section.

Conclusions

The backsplash of new particles during cratering (pitting) will far exceed the release of pre-existing contaminant particles. The backsplash source is estimated to be 6.9×10^5 to 1.4×10^7 particles (≥ 2 μm) per day or 2.0×10^5 to 3.3×10^5 particles (≥ 10 μ m) per day. The impact source is estimated at only 5.7×10^3 particles (≥ 5 μm) per day. Note that the impact source scales in the contamination level of particulates of size 5 μm or greater (taken as 10^6 m^{-2}). Backsplash produces mostly small particles (2-10 μm), with the estimate being very uncertain. Impact-released particles are fairly uniform in the size range 5-105 μm. Backsplash particles have high velocities ($\sim$500 m/s), with the larger particles proportionately slower. Impact-released particles have lower typical velocities ($\sim$3 cm/s), which are fairly independent of size.

It is interesting but difficult to compare these predictions with the obserations of particle tracks by the Skylab S-052 coronagraph. Simpson and Witteborn[13] inferred a particle source rate of 1.33 s^{-1} on this basis, with severe requirement on the direction of emission and the form of the particle trajectories. They also calculated a minimum detectable size of 6.6 μm, depending on transverse velocity. Given that Skylab has a total surface area similar to that of the Orbiter, but a solar panel area of only about 300 m^2, the predictions of the model presented here are 6.6×10^{-2} s^{-1} from impact release and 1.6-5.7 s^{-1} from backsplash. However, the detectable size/velocity dependence of the instrument[14] would render it blind to many of the fast backsplash particles. A revised estimate of the Skylab rate would be 0.3-3.4 s^{-1}, which bounds the value derived by Simpson and Witteborn.[13]

Acknowledgments

The author wishes to acknowledge the helpful criticism and information on useful reference works provided by J.P. Simpson (NASA Ames Research Center). The research described in this paper was carried out by the Jet Propulsion Laboratory, California Institute of Technology, under NASA Contract NAS7-100.

References

[1] Barengoltz, J. and Edgars, D., "The Relocation of Particulate Contamination During Spaceflight," Jet Propulsion Laboratory, Pasadena, Calif., TM 33-737, 1975.

[2] "Meteoroid Environment Model—1970 (Interplanetary and Planetary)," NASA SP-8038, 1970.

[3] Rolsten, R.F. and Hunt, H.H., "Dynamic Stress at Hypervelocity Impact and True Tensile Strength," *Canadian Aeronautics and Space Journal,* Vol. 13, June 1967, pp. 269-272.

[4] Ludloff, K.G., "A Hydrodynamic Model for Hypervelocity Impact," Ph.D. Thesis, UCLA, 1967.

[5] Gault, D.E. and Heitowit, E.D., "The Partition of Energy for Hypervelocity Impact Craters Formed in Rock," *Proceedings of Sixth Symposium on Hypervelocity Impact,* Vol. II, 1963, pp. 419-456..

[6] Herrmann, W. and Jones, A.H., "Correlation of Hypervelocity Impact Data," *Proceedings of the Fifth Symposium on Hypervelocity Impact,* Vol. I, Part 2, 1962, pp. 389-438.

[7] Christman, D.R. and Gehring, J.W., "Analysis of High-Velocity Projectile Penetration Mechanics," *Journal of Applied Physics,* Vol. 37, No. 4, March 1966, pp. 1579-1587.

[8] Bjork, R.L., "Review of Physical Processes in Hypervelocity Impact and Penetration," The Rand Corporation, Memorandum RM-3529-PR, 1963.

[9] Gault, D.E., "Displaced Mass, Depth, Diameter, and Effects of Oblique Trajectories for Impact Craters Formed in Dense Crystalline Rocks," *The Moon,* Vol. 6, Jan.-Feb. 1973, pp. 32-44.

[10] Mandeville, J.C. and Vedder, J.F., "Microcraters Formed in Glass by Low Density Projectiles," *Earth and Planetary Science Letters,* Vol. 11, No. 4, July 1971, pp. 297-306.

[11] Bjork, R.L., Kreyenhagen, K.N., and Wagner, M.H., "Analytical Study of Impact Effects as Applied to the Meteoroid Hazard," Shock Hydrodynamics, Inc., NASA CR-757, 1965.

[12] Eichelberger, R.J. and Gehring, J.W., "Effects of Meteoroid Impacts on Space Vehicles," *American Rocket Society Journal,* Vol. 32, Oct. 1962, pp. 1583-1591.

[13] Simpson, J.P. and Witteborn, F.C., "The Effect of the Shuttle Contaminant Environment on a Sensitive Infrared Telescope," *Applied Optics,* Vol. 16, Aug. 1977, pp. 2051-2073.

[14] Schuerman, D.W. and Weinberg, J.L., "Preliminary Study of Contaminant Particulates Around Skylab," NASA CR-2759, 1976.